Journal of Multidisciplinary Engineering Science and Technology (JMEST)
ISSN: 2458-9403
Vol. 11 Issue 11, November - 2024

Digital Microfluidic DNA Ligation on Low-Cost Ink-Jet Printed Devices

Sari Houchaimi[1] and Michael J. Schertzer[1]
[1]Department of Mechanical Engineering, Rochester Institute of Technology, Rochester, NY, USA

***Abstract*—This investigation demonstrates successful fabrication of digital microfluidic devices with inkjet-printed electrodes that are capable of performing the assembly of two small double stranded DNA products into one larger product. DNA assembly is a critical part of many biological applications including organism engineering, agricultural improvement, and gene therapy. Automation of this protocol using digital microfluidic devices may open a supply side bottleneck that causes a drag on innovation in these important applications. Digital microfluidic devices offer the promise of automating complex biological processes by individually manipulating small droplets of fluid without the use of channels, pumps, or valves. We test the use of low-cost inkjet-printed digital microfluidic devices by examining our yield in small batch fabrication of devices that use three different electrode geometries. We found that adding small interdigitations to square electrodes improved droplet mobility on these devices without reducing yield relative to plain square electrodes. We used the interdigitated electrode design to demonstrate DNA assembly on inkjet-printed digital microfluidic devices. Unfortunately, droplet creation was not repeatable on any of the devices tested. We believe this can be attributed to the relatively large gap distances required using this fabrication method to avoid creating short-circuits between neighboring electrodes on the device.**

Keywords—Digital Microfluidics; DNA Assembly; Electrowetting; Inkjet-Lab on a chip.

I. INTRODUCTION

Reliable generation of long, accurate, DNA products is of critical importance for a wide variety of biological applications such as targeting, delivery, and production of drugs [1], DNA data storage [2], production of biofuel [3], and synthetic biology [4]. Recent works have sought to improve reliability of DNA assembly with engineered enzymes that can reduce cycle time while producing large DNA products more accurately than conventional methods [4]–[9]. These methods tend to be aqueous (i.e., water-based) in nature and eliminate the commonly used solvent acetonitrile. This makes DNA assembly an attractive candidate for digital microfluidic (DMF) automation, because these devices have difficulty moving droplets with appreciable concentrations of acetonitrile [10].

DMF devices make use of electrowetting on dielectric (EWOD) droplet actuation to automate biological processes [11]–[14]. They manipulate nanoliter droplets of biomolecular cargo across an array of electrodes. Droplets are usually confined between an actuation layer and an upper plate with a large planar ground electrode. DMF devices create, move, mix, and split droplets across this two-dimensional electrode array without using channels, pumps, or valves [15]. They also allow real-time impedimetric sensing of droplet presence and composition.

We have made practical and theoretical contributions to electrowetting induced droplet detachment [16], [17], ink-jet printed DMF devices[17], DMF particle separations [18], real-time impedimetric sensing[19], [20], and DMF droplet manipulation and contact line dynamics [21]–[23].

DMF biomolecule capability has led to automation of many biomedical applications [24]–[26]. DMF provides automated, multiplexed, and reconfigurable solutions for complex multi-reagent processes that would be difficult to realize in channel-based devices without dramatically increasing fabrication complexity. These devices provide a compelling platform to perform a wide variety of biochemical applications including nucleic acid analysis and cell manipulation [27]–[29].

There have been a variety of attempts to reduce DMF device fabrication costs by moving device fabrication outside of the cleanrooms typically required for micro and nano fabrication. These investigations have focused on techniques such as microcontact printing [30], laser printing on printed circuit boards [31], and the use of photomasks drawn by hand [31].

Inkjet-printing has also been used to fabricate electrodes for DMF devices [32]–[36]. We believe these techniques provide an excellent combination of accessibility, affordability, accuracy, and repeatability. One of the disadvantages of this technique is reduced feature resolution. In DMF devices, the limiting resolution is generally the spacing between adjacent electrodes so that the contact line of the droplet overlaps with the neighboring electrodes after droplet actuation. Inkjet-printed devices reported in the literature have achieved resolutions on the order of $60\ \mu m$ to $100\ \mu m$ [34], [35].

The limitation caused by larger gap distances between electrodes in DMF devices can be at least

somewhat overcome by designing electrodes with interdigitated elements that cut into neighboring electrodes. Interdigitation of electrodes has been used in DMF devices since at least the early work of Pollack and Fair [37]. The star shaped electrodes used in Dixon et al. [34] also appear to be suitable for IJP DMF devices as they only require one overlapping feature between neighboring electrodes as opposed to the many interdigitated features in other works [37].

This investigation demonstrates the ligation of two small DNA products into one larger product on an inkjet-printed DMF device. To that end, we also explore various inkjet-printed electrode designs and report on repeatability of droplet creation and actuation using inkjet-printed interdigitated and star shaped electrodes.

II. Experimental Methods

A. Device Fabrication

Devices used in this investigation manipulate droplets confined between two substrates (Fig. 1). The upper substrate consists of a glass slide coated with the transparent conductor indium tin oxide (ITO). This layer is made hydrophobic by spin-coating a thin film of Teflon AF (~ $100\,nm$) following methods recommended by the manufacturer.

The lower substrate was fabricated in the same manner as in our previous work [35]. This component consists of ink-jet printed electrodes patterned on a flexible media and spin-coated dielectric and hydrophobic layers. After printing, media is bonded to a glass slide using double sided Kapton tape and allowed to cure at room temperature for approximately 24 hours. It then undergoes a three-step spin-coating process. First, the printed layer is coated with a thin layer of Teflon (~ $100\,nm$). This layer was found to improve adhesion between the media and the dielectric layer. Then, an SU8 3005 (viscosity of $65\,cst$) dielectric layer (~ $4.4\,\mu m$) is spun onto the surface. Finally, a hydrophobic layer of Teflon (~ $100\,nm$) is spun onto the device. All spin coating procedures were performed following parameters recommended by the manufacturer.

Electrodes were printed on a transparent flexible PET based media (Novacentrix Novele) using an Epson C88+ Stylus printer using Novacentrix JS-B25P silver nanoink with particle sizes of $83\,nm$ as described in [34], [35]. The following print settings were applied: paper type *premium glossy photo paper*; print quality *best*, and image type *line art*. Gaps between electrodes in print files were set at $200\,\mu m$ to electrically connecting neighboring electrodes, but gaps between printed features are reported to be smaller than those specified in the associated print files [34]. Multiple electrode patterns were explored to determine which patterns provided more consistent droplet actuation.

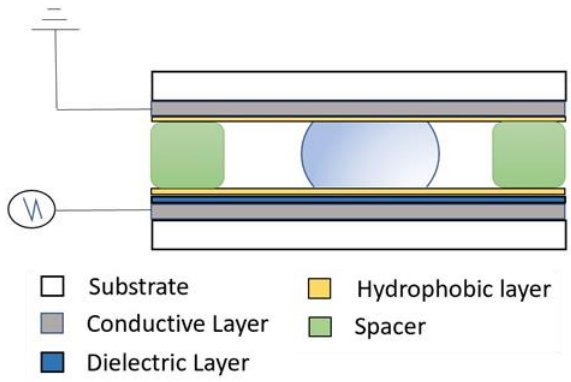

Fig. 1. Schematic representation of a DMF device confining droplet of reagent between two substrates.

B. Experimental Facility

The experimental facility used in this investigation consists of the DMF device (described in A) and a control system. The control system consists of a National Instruments PXI 1033 chassis that includes a signal generator (NI PXI 4502) and matrix switching card (NI PXI 2529) similar to our previous work [16], [19], [35], [38]. An actuation signal with frequencies of $1\,kHz$ or $10\,kHz$ was generated by the signal generator and amplified up to a voltage on the order of $100\,V_{rms}$ using a Trek PZD700A amplifier. This voltage was applied to target actuation electrodes on the DMF device using custom NI LabVIEW software to control the switching card similar to our previous work [18], [19], [39].

The DMF device was connected to the control system using a pogo pin board acquired from the Wheeler microfluidics lab at a DropBot workshop. This board was attached to a 3D printed fixture that aligned the board and the DMF device.

Images of the DMF device during operation were captured using a Zeiss stereo discovery V8 microscope with an attached Zeiss axiocam Mrm.

C. Ligation Assay

In this investigation, all experiments assemble two double-stranded DNA oligonucleotides that will be referred to as “bricks”. Each brick is made up of three oligonucleotides (Integrated DNA Technologies) of smaller approximately 80 nucleotides. Oligonucleotides 1A, 1B, and 1C hybridize to form DNA Brick 1, and 2A, 2B, and 2C hybridize to form DNA Brick 2. These oligonucleotides, at a strand concentration of 5 μM, were annealed without ligation at 85 °C for 5 minutes in 1x T4 DNA ligase buffer (New England Biolabs) and subsequently snap-cooled on ice for 30 minutes. This process occurred off-chip.

DNA assembly occurred on-chip and in benchtop controls. Bricks were first ligated on bench using the following mixture: 10.5 μL of nuclease-free water, 1.2 μL of T4 DNA ligase buffer (10X), 4.0 μL of Brick 1 (5 μM), 4.1 μL of Brick 2 (5 μM) and 0.2 μL of T4 DNA ligase. Following the ligation on bench, the mixture was first incubated for 60 minutes at room temperature. Proteinase K and calcium chloride were added before incubations at 30 minutes at 37 ºC and 10 minutes at 70 ºC.

This protocol was then adapted for IJP DMF devices. A surfactant was necessary in the DMF procedure to prevent biofouling and facilitate droplet movement, as proteins and other biological materials tend to adhere to the device surface. Tween 20 was used at a concentration of 0.1% per volume. A stock solution for each brick was made with the following proportions: 5 μL Brick solution in ligase buffer, 2.5 μL of Tween solution (1%), and 17.5 μL of nuclease-free water.

The size of products assembled on bench and on DMF were measured using gel electrophoresis. A 2% agarose gel was run at 100 V for approximately 50 minutes with an ethidium bromide protocol. Results were visualized using a Chemidoc XRS+ (Bio-Rad).

III. Results and Discussion

A. Electrode geometry

We examined three potential electrode configurations to determine print yield and reliability of creation and manipulation on DMF devices with inkjet-printed electrodes (square, interdigitated, and star shaped electrodes). Initial testing suggested that printing devices with gap distances between electrodes less than 200 μm in the layout file led to low yields due to shorting of adjacent electrodes across all

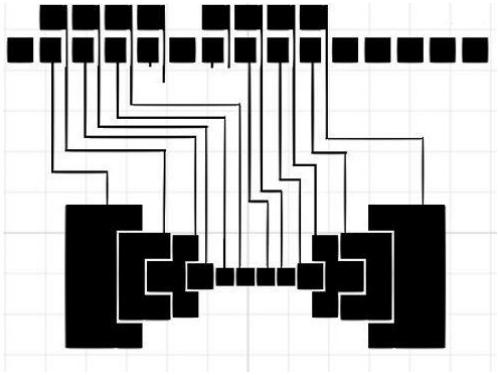

Fig. 2. Electrode layout for TTC Square inkjet printed digital microfluidic devices.

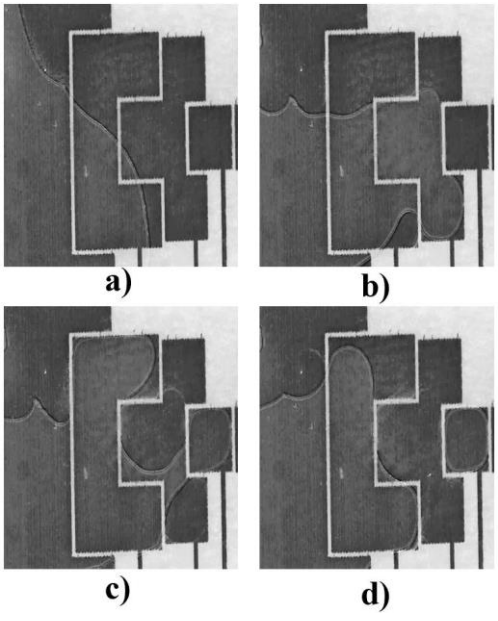

Fig. 3. Experimental images showing an example of successful droplet creation on an inkjet printed DMF device with the TTC square electrode design. Images show (a-b) droplet dispensing, (c) droplet necking, and (d) droplet splitting.

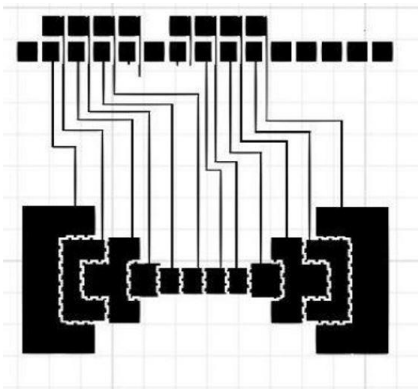

Fig. 4. Electrode layout for TTC interdigitated square inkjet-printed digital microfluidic devices.

three design types. For square and interdigitated electrodes, we adopted the TTC electrode geometry proposed by Nikapitiya et al. as it had been shown to reliably create droplets on cleanroom-fabricated

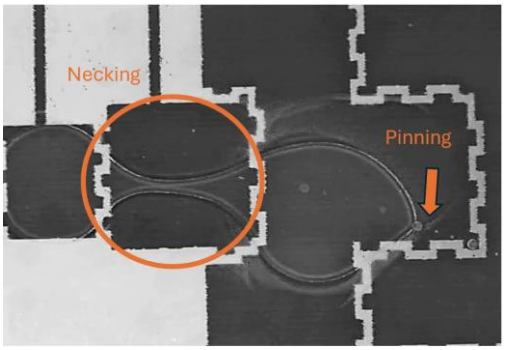

Fig. 5. Experimental image showing knecking on an interdigitated TTC inkjet-printed digital microfluidic device. While droplet necking was observed, creation was not. This image also shows the droplet pinning that could occur on these devices. Likely due to non-homogeneities on the surface due to the low-cost inkjet printing fabrication method.

devices [40]. For the star shaped electrodes, we adopted the design proposed by Dixon et al. where the first dispensing electrode penetrates the reservoir electrode [34].

Our initial tests were performed on devices with square electrodes with TCC reservoir electrodes for droplet creation (Fig. 2). We printed 12 devices with this configuration. Seven of these devices were free of shorts such that each electrode in the system was individually addressable (58.3%). All these devices were tested for droplet mobility and creation. While droplet mobility was observed on these devices using both $1\,kHz$ and $10\,kHz$ signals, it tended to be inconsistent. Droplet creation was observed in some cases (Fig. 3), but was not consistent.

To promote more consistent droplet movement, we tested a design with interdigitated square electrodes (Fig. 4). We printed 24 of these devices, and 14 of them were free of shorted electrodes (58%). The similar failure rate observed between prints of square and interdigitated designs suggests that the increased complexity did not cause an appreciable increase in failure due to electrode shorting. The 14 successfully

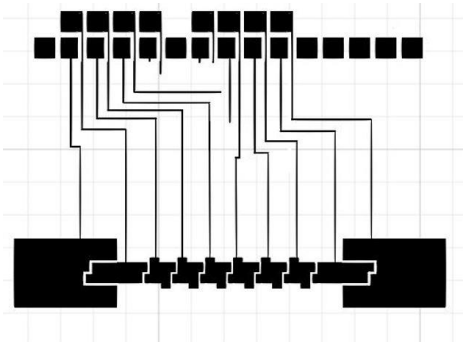

Fig. 6. Experimental image showing knecking on an interdigitated TTC inkjet-printed digital microfluidic device. Whild droplet necking was observed, creation was not. This image also shows the droplet pinning that could occur on these devices. Likely due to non-homogeneities on the surface due to the low-cost inkjet printing fabrication method.

printed devices were tested for droplet mobility and creation. While we observed more consistent movement between neighboring electrodes in the center of the device, droplet creation was not observed in these tests using either actuation frequency. In the most common failure mode, a finger of fluid was successfully withdrawn from the reservoir and fluid was pulled back on the TTC array causing necking in the fluid (Fig. 5). Unfortunately, droplet splitting was not observed in these cases.

The third inkjet-printed electrode design we tested was the star pattern proposed by Dixon et al. [34] (Fig. 6). Unfortunately, there were no devices that were free of short-circuits among the 12 devices we printed using this design. It is likely that this high failure rate is the result of the larger gap widths used in this investigation compared to Dixon et al. [34]. While we followed the same reported process (e.g. printer, ink, media, settings), we could not repeatably print patterns with individually addressable electrodes for gap distances below the $200\ \mu m$ reported here. We had no successful prints at the $60\ \mu m$ gap width reported by Dixon et al. [34].

The goal of electrode geometry testing was to find the most reliable pattern for droplet movement in DNA ligation testing. Consequently, the "TCC interdigitated square" design was adopted for this experiment.

B. DNA Ligation

A benchtop control was performed before performing DNA ligation on inkjet-printed DMF devices. This control mixed and incubated the same short (~ 125 base pair) DNA bricks and assembled them using traditional benchtop methods. As seen in Figure 7, the result of this benchtop ligation is a single product with a size of approximately 250 base pairs. After validating this protocol on the bench, we proceeded to perform DNA ligation on an inkjet-printed DMF device.

Inkjet-printed DMF devices with interdigitated electrodes were selected to perform DNA assembly in this investigation as this design provided the highest droplet mobility of the layouts examined here. In these tests, stock solutions containing Bricks 1 and 2 were created off-chip and loaded onto the device before confining them by adding the top plate of the device. Droplets were then merged and incubated at room temperature on the device (Fig. 8). The merged droplet was harvested from the device to undergo off-chip incubations at $37\ °C$ and $70\ °C$. The size of the on-chip

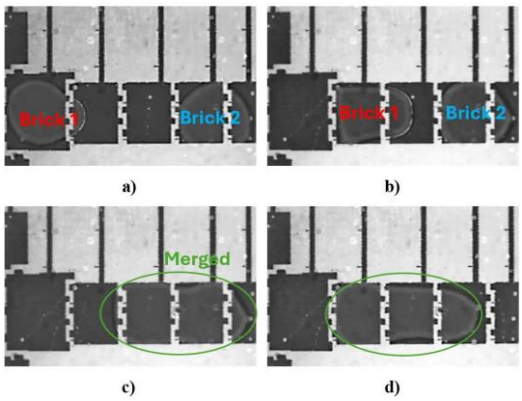

Fig. 8. Experimental images demonstrating (a-b) manipulation and (c-d) merger of droplets containing DNA bricks 1 and 2 on an inkjet-printed DMF device with interdigitated square electrodes.

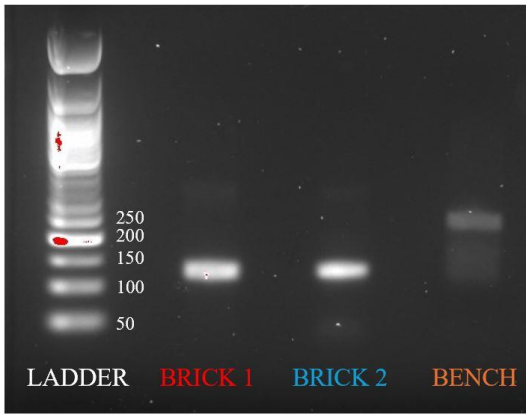

Fig. 7. Image of an electrophoretic gel showing the size of the two DNA bicks (BRICK 1 and BRICK 2) and the product of ligation following the benchtop ligation protocol (BENCH).

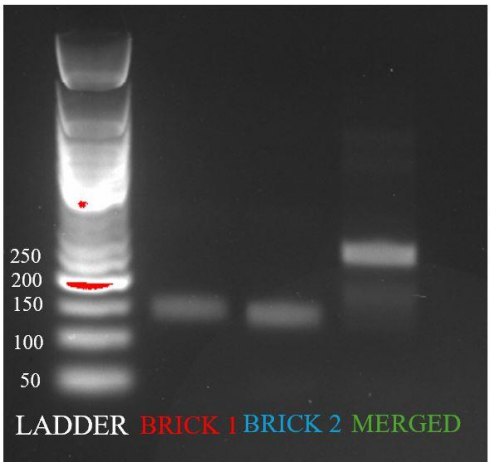

Fig. 9. Image of an electrophoretic gel showing the size of the two DNA bicks (BRICK 1 and BRICK 2) and the product of logation on an inkjet-printed DMF device with interdigitated square electrodes.

DNA product was found to be approximately 250 base pairs, which agreed with the benchtop control (Fig. 9).

This suggests that the DNA assembly method used here is suitable for digital microfluidic automation in inkjet-printed devices. However, higher resolution prints are likely necessary to achieve more robust droplet creation and manipulation.

IV. Conclusion

We present the successful ligation of double-stranded DNA products on an inkjet-printed digital microfluidic device. These devices consisted of two substrates with inkjet-printed electrodes spaced 200 μm apart.

Three electrode designs were examined to test for successful printing and for DMF droplet creation and movement. Devices using square and interdigitated square electrodes used a TCC pattern from the literature which has been previously shown to produce robust droplet creation on cleanroom-fabricated devices. A star electrode pattern from a previous investigation using inkjet-printed electrodes was also tested. Almost 60% of printed patterns were successful when using square and interdigitated square electrode patterns. Square electrodes were found to provide intermittent movement and creation. Interdigitated square electrodes improved consistency of droplet movement, but did not successfully create droplets despite being able to draw fluid from reservoirs. Unfortunately, none of the devices we printed with star-shaped patterns were free of short-circuited electrodes.

Two DNA bricks were ligated into one larger DNA product on benchtop and on IJP DMF device with interdigitated square electrodes. Gel electrophoresis results show that the same product size was obtained on both platforms. This suggests that IJP DMF devices can be used to automate DNA ligation.

This opens the possibility of fabricating low-cost DMF devices outside the cleanroom to automate biological protocols. The drawbacks of this technique were (i) neighboring electrodes in the printed pattern were often electrically connected and (ii) inconsistent splitting of droplets on the device. We hypothesize that both of these issues would be resolved by using printing techniques that can reliably create gaps between electrodes smaller than 200 μm.

Acknowledgement

The authors gratefully acknowledge the support of the Kate Gleason College of Engineering and the Department of Mechanical Engineering at the Rochester Institute of Technology.

References

[1] A. S. Khalil and J. J. Collins, “Synthetic biology: Applications come of age,” *Nature Reviews Genetics*. 2010.

[2] H. H. Lee, R. Kalhor, N. Goela, J. Bolot, and G. M. Church, “Terminator-free template-independent enzymatic DNA synthesis for digital information storage,” *Nat. Commun.*, 2019.

[3] S. C. C. Shih *et al.*, “A Versatile Microfluidic Device for Automating Synthetic Biology,” *ACS Synth. Biol.*, 2015.

[4] M. A. Jensen and R. W. Davis, “Template-Independent Enzymatic Oligonucleotide Synthesis (TiEOS): Its History, Prospects, and Challenges,” *Biochemistry*, vol. 57, no. 12, pp. 1821–1832, 2018.

[5] S. Palluk *et al.*, “De novo DNA synthesis using polymerasenucleotide conjugates,” *Nat. Biotechnol.*, vol. 36, no. 7, pp. 645–650, 2018.

[6] S. Barthel, S. Palluk, N. J. Hillson, J. D. Keasling, and D. H. Arlow, “Enhancing terminal deoxynucleotidyl transferase activity on substrates with 3′ terminal structures for enzymatic De Novo DNA synthesis,” *Genes (Basel).*, vol. 11, no. 1, pp. 1–9, 2020.

[7] M. Hao, J. Qiao, and H. Qi, “Current and emerging methods for the synthesis of single-stranded DNA,” *Genes (Basel).*, vol. 11, no. 2, 2020.

[8] H. Lee *et al.*, “Photon-directed multiplexed enzymatic DNA synthesis for molecular digital data storage,” *Nat. Commun.*, vol. 11, no. 1, pp. 1–9, 2020.

[9] E. Yoo, D. Choe, J. Shin, S. Cho, and B. K. Cho, “Mini review: Enzyme-based DNA synthesis and selective retrieval for data storage,” *Comput. Struct. Biotechnol. J.*, vol. 19, pp. 2468–2476, 2021.

[10] R. B. Fair, “Digital microfluidics: Is a true lab-on-a-chip possible?,” *Microfluid. Nanofluidics*, vol. 3, pp. 245–281, 2007.

[11] M. Washizu, “Electrostatic actuation of liquid droplets for microreactor applications,” *IEEE Trans. Ind. Appl.*, vol. 34, no. 4, pp. 732–737, 1998.

[12] R. B. Fair *et al.*, “Chemical and Biological Applications of Digital-Microfluidic Devices,” *IEEE Des. Test Comput.*, vol. 24, no. 1, pp. 10–24, 2007.

[13] W. C. Nelson and C.-J. Kim, “Droplet Actuation by Electrowetting-on-Dielectric (EWOD): A Review,” *J. Adhes. Sci. Technol.*, vol. 26, no. 12–17, pp. 1747–1771, 2012.

[14] M. J. Jebrail, M. S. Bartsch, and K. D. Patel, “Digital microfluidics: A versatile tool for applications in chemistry, biology and medicine,” *Lab Chip*, vol. 12, no. 14, pp. 2452–2463, 2012.

[15] S. K. Cho, H. Moon, and C. J. Kim, “Creating, transporting, cutting, and merging liquid droplets by electrowetting-based actuation for digital microfluidic circuits,” *J. Microelectromechanical Syst.*, vol. 12, no. 1, pp. 70–80, 2003.

[16] C. T. Burkhart, K. L. Maki, and M. J. Schertzer, “Coplanar Electrowetting-Induced Droplet Detachment from Radially Symmetric

Electrodes," *Langmuir*, vol. 36, no. 28, pp. 8129–8136, 2020.

[17] K. A. Bernetski, C. T. C. T. Burkhart, K. L. Maki, and M. J. M. J. M. J. Schertzer, "Characterization of Electrowetting, Contact Angle Hysteresis, and Adhesion on Digital Microfluidic Devices with Inkjet-Printed Electrodes," *Microfluid. Nanofluidics*, vol. 22, no. 96, pp. 1–10, 2018.

[18] M. J. Schertzer, R. Ben-Mrad, and P. E. Sullivan, "Mechanical Filtration of Particles in Electrowetting on Dielectric Devices," *J. Microelectromechanical Syst.*, vol. 20, no. 4, pp. 1010–1015, Aug. 2011.

[19] M. J. Schertzer, R. Ben-Mrad, and P. E. Sullivan, "Using capacitance measurements in EWOD devices to identify fluid composition and control droplet mixing," *Sensors Actuators B Chem.*, vol. 145, no. 1, pp. 340–347, Mar. 2010.

[20] E. Scott-Murrell, D. Lanza, and M. J. Schertzer, "Dimensionless model for impedimetric sensing of particle laden droplets in digital microfluidic devices," *Microsyst. Technol.*, vol. 23, no. 8, pp. 3131–3139, 2017.

[21] M. J. Schertzer, S. I. Gubarenko, R. Ben Mrad, and P. E. Sullivan, "An empirically validated model of the pressure within a droplet confined between plates at equilibrium for low Bond numbers," *Exp. Fluids*, vol. 48, no. 5, pp. 851–862, Nov. 2009.

[22] M. J. Schertzer, S. I. Gubarenko, R. Ben-Mrad, and P. E. Sullivan, "An empirically validated analytical model of droplet dynamics in electrowetting on dielectric devices," *Langmuir*, vol. 26, no. 24, pp. 19230–19238, Dec. 2010.

[23] K. A. Bernetski, K. L. Maki, and M. J. Schertzer, "Comment on 'How to make sticky surfaces slippery: Contact angle hysteresis in electrowetting with alternating voltage' [Appl. Phys. Lett. 114 , 116101 (2019)]," *Appl. Phys. Lett.*, vol. 114, no. 11, p. 116102, 2019.

[24] X. Xu *et al.*, "Digital microfluidics for biological analysis and applications," *Lab on a Chip*. 2023.

[25] K. Choi, A. H. C. Ng, R. Fobel, and A. R. Wheeler, "Digital microfluidics.," *Annu. Rev. Anal. Chem. (Palo Alto. Calif).*, vol. 5, pp. 413–40, Jan. 2012.

[26] J. Li and C. J. Kim, "Current commercialization status of electrowetting-on-dielectric (EWOD) digital microfluidics," *Lab Chip*, vol. 20, no. 10, pp. 1705–1712, 2020.

[27] X. Liu *et al.*, "Electrowetting-based digital micro fluidics : Toward a full-functional miniaturized platform for biochemical and biological applications," *Trends Anal. Chem.*, vol. 166, p. 117153, 2023.

[28] R. Shen *et al.*, "Nucleic acid analysis on electrowetting-based digital microfluidics," *TrAC - Trends in Analytical Chemistry*. 2023.

[29] L. Pang, J. Ding, X. X. Liu, and S. K. Fan, "Digital microfluidics for cell manipulation," *TrAC - Trends in Analytical Chemistry*, vol. 117. Elsevier B.V., pp. 291–299, 01-Aug-2019.

[30] M. W. L. Watson, M. Abdelgawad, G. Ye, N. Yonson, J. Trottier, and A. R. Wheeler, "Microcontact printing-based fabrication of digital microfluidic devices," *Anal. Chem.*, vol. 78, no. 22, pp. 7877–7885, 2006.

[31] M. Abdelgawad and A. R. Wheeler, "Low-cost, rapid-prototyping of digital microfluidics devices," *Microfluid. Nanofluidics*, vol. 4, no. 4, pp. 349–355, Jul. 2007.

[32] H. Ko *et al.*, "Active digital microfluidic paper chips with inkjet-printed patterned electrodes," *Adv. Mater.*, vol. 26, no. 15, pp. 2335–2340, 2014.

[33] R. Fobel, A. E. Kirby, A. H. C. Ng, R. R. Farnood, and A. R. Wheeler, "Paper microfluidics goes digital.," *Adv. Mater.*, vol. 26, no. 18, pp. 2838–43, May 2014.

[34] C. Dixon, A. H. C. Ng, R. Fobel, M. B. Miltenburg, and A. R. Wheeler, "An inkjet printed, roll-coated digital microfluidic device for inexpensive, miniaturized diagnostic assays," *Lab Chip*, vol. 16, no. 23, pp. 4560–4568, 2016.

[35] K. Bernetski, C. T. Burkhart, K. L. Maki, and M. J. Schertzer, "Characterization of Electrowetting, Contact Angle Hysteresis, and Adhesion on Digital Microfluidic Devices with Inkjet-Printed Electrodes," *Microfluid. Nanofluidics*, vol. 22, no. 96, pp. 1–10, 2018.

[36] H. Wang and L. Chen, "Novel electrodes for precise and accurate droplet dispensing and splitting in digital microfluidics," *Nanotechnol. Rev.*, 2021.

[37] M. G. Pollack and R. B. Fair, "Electrowetting-based actuation of liquid droplets for microfluidic applications," *Appl. Phys. Lett.*, vol. 77, no. 11, pp. 1725–1726, 2000.

[38] K. A. Bernetski, H. T. An, K. L. Maki, and M. J. Schertzer, "Predicting actuated contact line pinning forces and the elimination of hysteresis under AC electrowetting," *Microfluid. Nanofluidics*, vol. 26, no. 12, pp. 1–8, 2022.

[39] M. J. Schertzer, R. Ben Mrad, and P. E. Sullivan, "Automated detection of particle concentration and chemical reactions in EWOD devices," *Sensors Actuators B Chem.*, vol. 164, no. 1, pp. 1–6, Mar. 2012.

[40] N. Y. J. B. Nikapitiya, S. M. You, and H. Moon, "Droplet dispensing and splitting by electrowetting on dielectric digital microfluidics," *Proceedings of the IEEE International Conference on Micro Electro Mechanical Systems (MEMS)*, pp. 955–958, 2014, doi: 10.1109/MEMSYS.2014.6765801.